Deep-inelastic Production of Heavy Quarks

E. Laenen[a], M. Buza[b], B.W. Harris[c], Y. Matiounine[d], R. Migneron[e], S. Riemersma[f], J. Smith[d], W.L. van Neerven[g]

[a] CERN Theory Division, CH-1211 Geneva 23, Switzerland
[b] NIKHEF, PO Box 41882, NL-1009 DB Amsterdam, The Netherlands
[c] Physics Department, Florida State University, Tallahassee, FL 32306-3016, USA
[d] Institute for Theoretical Physics, SUNY Stony Brook, NY 11794, USA
[e] Dept. of Applied Math., University of Western Ontario, London, Ontario, N6A 5B9, Canada
[f] DESY IfH-Zeuthen, Platanenallee 6, D-15735 Zeuthen, Germany
[g] Instituut Lorentz, University of Leiden, PO Box 9506, NL-2300 RA Leiden, The Netherlands

Abstract: Deep-inelastic production of heavy quarks at HERA, especially charm, is an excellent signal to measure the gluon distribution in the proton at small x values. By measuring various differential distributions of the heavy quarks this reaction permits additional more incisive QCD analyses due to the many scales present. Furthermore, the relatively small mass of the charm quark, compared to the typical momentum transfer Q, allows one to study whether and when to treat this quark as a parton. This reaction therefore sheds light on some of the most fundamental aspects of perturbative QCD. We discuss the above issues and review the feasibility of their experimental investigation in the light of a large integrated luminosity.

1 Introduction

Since the previous HERA workshop in 1991 significant progress has been made on the theoretical side in understanding the production of heavy quarks in electron proton collisions. Improvements in available experimental techniques and particularly the expected increase in luminosity amply justify this effort. In general the progress consists of the calculation of all $O(\alpha_s)$ corrections to the processes of interest, thus improving the accuracy of the theoretical predictions both in shape and normalization. At the time of the previous workshop the only NLO calculations available were for the case of inclusive photoproduction [1]. In the meantime NLO calculations have also been performed for inclusive electroproduction [2, 3, 4], and both have been extended to the fully differential cases [5, 6, 7]. Therefore, meaningful and extensive comparisons between theory and data can now be made. In what follows we review how the deeply inelastic electroproduction process allows us to explore, in detail, three areas of perturbative QCD in particular.

We first discuss the inclusive case, via the structure function $F_2(x,Q^2,m^2)$. We show that this structure function for the case of charm suffers from only very modest theoretical uncertainty, that its NLO corrections are not too large, and that it is sensitive to the shape of the small-x gluon density. Next we treat single particle differential distributions in the charm kinematical variables, and also charm-anticharm correlations. Because many distributions can be studied, many QCD tests can be performed. Examples are tests of the production mechanism (boson-gluon fusion), studies of gluon radiation patterns, and dependence on scales such as deep-inelastic momentum transfer Q, the heavy quark mass m (with enough luminosity one can detect a sizable sample of bottom quarks), the transverse momentum of the charm quark, etc. Finally, in the last subsection, we review the theoretical status of the boson-gluon fusion description of charm production at small and very large Q. In essence, it involves answering the question: when is charm a parton?

2 Structure Functions and Gluon Density

This subsection has some overlap with the more detailed review on heavy flavour structure functions in the structure function section. Here we only present the most salient features. The reaction under study is

$$e^-(p_e) + P(p) \to e^-(p'_e) + Q(p_1)(\bar{Q}(p_1)) + X\,, \tag{1}$$

where $P(p)$ is a proton with momentum p, $Q(p_1)(\bar{Q}(p_1))$ is a heavy (anti)-quark with momentum p_1 ($p_1^2 = m^2$) and X is any hadronic state allowed. Its cross section may be expressed as

$$\frac{d^2\sigma}{dx dQ^2} = \frac{2\pi\alpha^2}{x\,Q^4}\left[(1+(1-y)^2)F_2(x,Q^2,m^2) - y^2 F_L(x,Q^2,m^2)\right]\,, \tag{2}$$

where

$$q = p_e - p'_e\,, \qquad Q^2 = -q^2\,, \qquad x = \frac{Q^2}{2p\cdot q}\,, \qquad y = \frac{p\cdot q}{p\cdot p_e}\,. \tag{3}$$

The inclusive structure functions F_2 and F_L were calculated to next-to-leading order (NLO) in Ref. [2]. The results can be written as

$$\begin{aligned} F_k(x,Q^2,m^2) \;=\; & \frac{Q^2\alpha_s}{4\pi^2 m^2}\int_x^{z_{\max}}\frac{dz}{z}\Big[\,e_H^2 f_g(\frac{x}{z},\mu^2)c_{k,g}^{(0)}\,\Big] \\ & +\frac{Q^2\alpha_s^2}{\pi m^2}\int_x^{z_{\max}}\frac{dz}{z}\Big[\,e_H^2 f_g(\frac{x}{z},\mu^2)(c_{k,g}^{(1)}+\bar{c}_{k,g}^{(1)}\ln\frac{\mu^2}{m^2}) \\ & +\sum_{i=q,\bar{q}}\Big[e_H^2\, f_i(\frac{x}{z},\mu^2)(c_{k,i}^{(1)}+\bar{c}_{k,i}^{(1)}\ln\frac{\mu^2}{m^2}) + e_{L,i}^2\, f_i(\frac{x}{z},\mu^2)d_{k,i}^{(1)}\,\Big]\Big]\,, \end{aligned} \tag{4}$$

where $k = 2, L$ and the upper boundary on the integration is given by $z_{\max} = Q^2/(Q^2 + 4m^2)$. The functions $f_i(x,\mu^2)\,, (i = g,q,\bar{q})$ denote the parton densities in the proton and μ stands for the mass factorization scale, which has been put equal to the renormalization scale. The $c_{k,i}^{(l)}(\eta,\xi)\,, \bar{c}_{k,i}^{(l)}(\eta,\xi)\,, (i = g\,,q\,,\bar{q}\,; l = 0,1)$ and $d_{k,i}^{(l)}(\eta,\xi)$, $(i = q\,,\bar{q}\,; l = 0,1)$ are coefficient functions and are represented in the $\overline{\rm MS}$ scheme. They depend on the scaling variables η and ξ defined by

$$\eta = \frac{s}{4m^2} - 1 \qquad\qquad \xi = \frac{Q^2}{m^2}\,. \tag{5}$$

where s is the square of the c.m. energy of the virtual photon-parton subprocess which implies that in (4) $z = Q^2/(Q^2+s)$. In eq. (4) we distinguished between the coefficient functions with respect to their origin. The coefficient functions indicated by $c_{k,i}^{(l)}(\eta,\xi)$, $\bar{c}_{k,i}^{(l)}(\eta,\xi)$ originate from the partonic subprocesses where the virtual photon is coupled to the heavy quark, whereas the quantity $d_{k,i}^{(l)}(\eta,\xi)$ comes from the subprocess where the virtual photon interacts with the light quark. Hence the former are multiplied by the charge squared of the heavy quark e_H^2, and the latter by the charge squared of the light quark e_L^2 respectively (both in units of e). Terms proportional to $e_H e_L$ integrate to zero for the inclusive structure functions. Furthermore we have isolated the factorization scale dependent logarithm $\ln(\mu^2/m^2)$. A fast program using fits to the coefficient functions [8] is available.

The first thing to note about eq. (4) is that the lowest order term contains only the gluon density. Light quark densities only come in at next order, and this is the reason $F_2(x,Q^2,m^2)$ is promising as a gluon probe. To judge its use as such, we must examine some of the characteristics of this observable. These are: the size of the $O(\alpha_s)$ corrections, the scale dependence, the mass dependence, its sensitivity to different gluon densities, and the relative size of the light quark contribution. These are the issues we investigate in this subsection. We take the charm mass 1.5 GeV, the bottom mass 5 GeV, the factorization scale equal to $\sqrt{Q^2+m^2}$ and choose at NLO the CTEQ4M [9] set of parton densities, with a two-loop running coupling constant for five flavors and $\Lambda = 202$ MeV, and at LO the corresponding CTEQ4L set, with a one-loop running coupling with five flavors and $\Lambda = 181$ MeV. In Fig. 1 we display $F_2(x,Q^2,m^2)$ vs. x

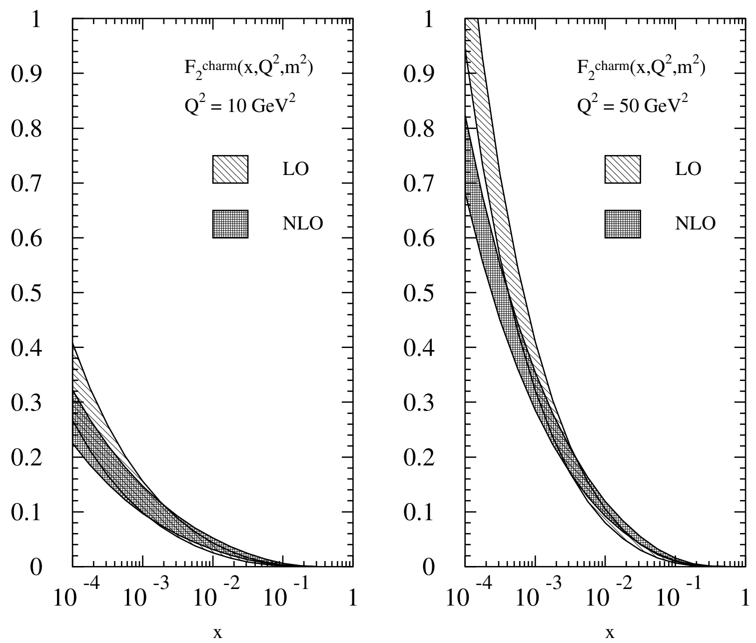

Figure 1: *$F_2(x,Q^2,m^2)$ vs. x at LO and NLO for two values of Q^2. The shaded areas indicate the uncertainty due to varying the charm mass from 1.3 to 1.7 GeV.*

for two values of Q^2 at LO and NLO. The scale dependence is much reduced by including the NLO corrections (when varying μ from 2 to 1/2 times the default choice, the structure function varies from, at LO, at most 20% and 13% at $Q^2 = 10$ and 50 GeV^2 respectively, to at most 5%

and 3% at NLO), but the dominant uncertainty is due to the charm mass and stays roughly constant, amounting at NLO maximally to about 16% for $Q^2 = 10$ GeV^2 and 10% for $Q^2 = 50$ GeV^2. The feature that the LO result is mostly larger than the NLO ones is due to the use of LO parton densities and one-loop α_s, and scale choice. Had we used NLO densities and a two-loop α_s, or chosen the scale μ equal to m, the LO result would have been below the NLO result. In the first case the size of the corrections is then about 40% at the central values at $Q^2 = 10$ GeV^2, and 25% at $Q^2 = 50$ GeV^2, and in the second case, at small x, about 20% and 30% respectively. In the next figure, Fig. 2, we show for the same values of Q^2 an important

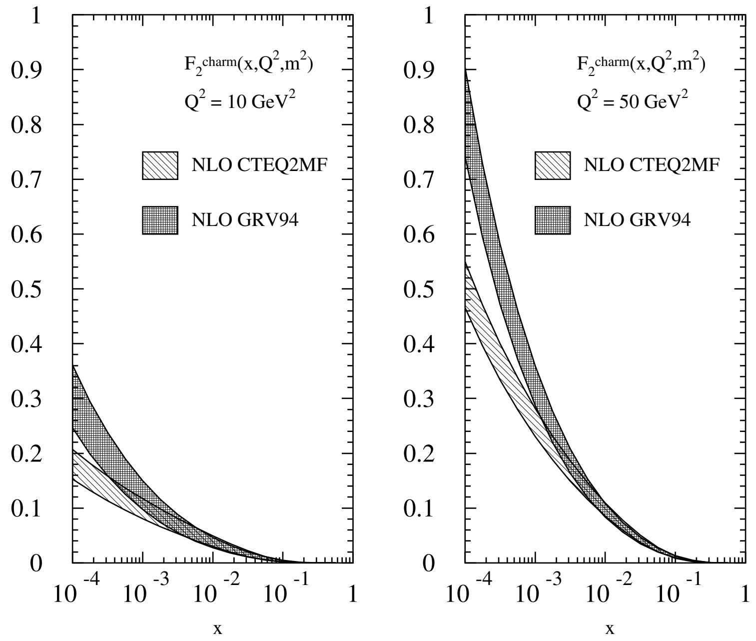

Figure 2: $F_2(x, Q^2, m^2)$ *vs.* x *at NLO for two choices of parton densities. The shaded areas again indicate the uncertainty due to varying the charm mass from 1.3 to 1.7 GeV.*

property, namely the sensitivity of the NLO F_2 to different parton density parametrizations. In this case we compare the CTEQ2MF set [10], whose gluon density stays quite flat when x becomes small, and the GRV94 set [11], which has a steeply rising gluon density. One sees that the difference is visible in the structure function. Finally we remark that the contribution of light quarks to the charm structure function is typically less than 5%. The bottom quark structure function is suppressed by electric charge and phase space effects and amounts to less than 2% (5%) at $Q^2 = 10\,(50)$ GeV^2 of the charm structure function. Previous investigations of the scale and parton density dependence of F_2 using the same NLO computer codes are available in [12] and [13].

We conclude that $F_2(x, Q^2, m^2)$ for charm production is an excellent probe to infer the gluon density in the proton at small x. The NLO theoretical prediction suffers from fairly little uncertainty, and the QCD corrections are not too large. See the section on structure functions in these proceedings for many more details, where also a comparison with (preliminary) data is shown. Therefore in view of a large integrated luminosity, a theoretically well-behaved observable, and promising initial experimental studies [14, 15] a precise measurement at HERA of the gluon density should be possible.

3 Single Particle Distributions and Heavy Quark Correlations

In this subsection we leave the fully inclusive case and examine in more detail the structure of the final state of the reaction

$$e^-(p_e) + P(p) \to e^-(p_e') + Q(p_1) + \bar{Q}(p_2) + X\,. \tag{6}$$

By studying various differential distributions of the heavy quarks we can learn more about the dynamics of the production process than from the structure function alone.

Single particle distributions $dF_2(x, Q^2, m^2, v)/dv$, where v is the transverse momentum p_T or rapidity y of the charm quark, were presented in NLO in [4] for various choices of x and Q^2. The LO distributions differed significantly from the NLO ones, so that the effect of $O(\alpha_s)$ corrections on such distributions cannot be described by a simple K-factor.

The $O(\alpha_s)$ corrections to $F_k(x, Q^2, m^2)$ in a fully differential form were calculated in Ref. [6] using the subtraction method. Recently [7], these fully differential structure functions were incorporated in a Monte-Carlo style program resulting in the $O(\alpha_s)$ corrections for reaction (6). The program for the full cross section, generated according to Eq. (2), allows one to study correlations in the lab frame. The phase space integration is done numerically. Therefore, it is possible to implement experimental cuts. It furthermore allows the use of a Peterson type fragmentation function. For details about the calculational techniques we refer to Ref. [6, 7]. Here we show mainly results.

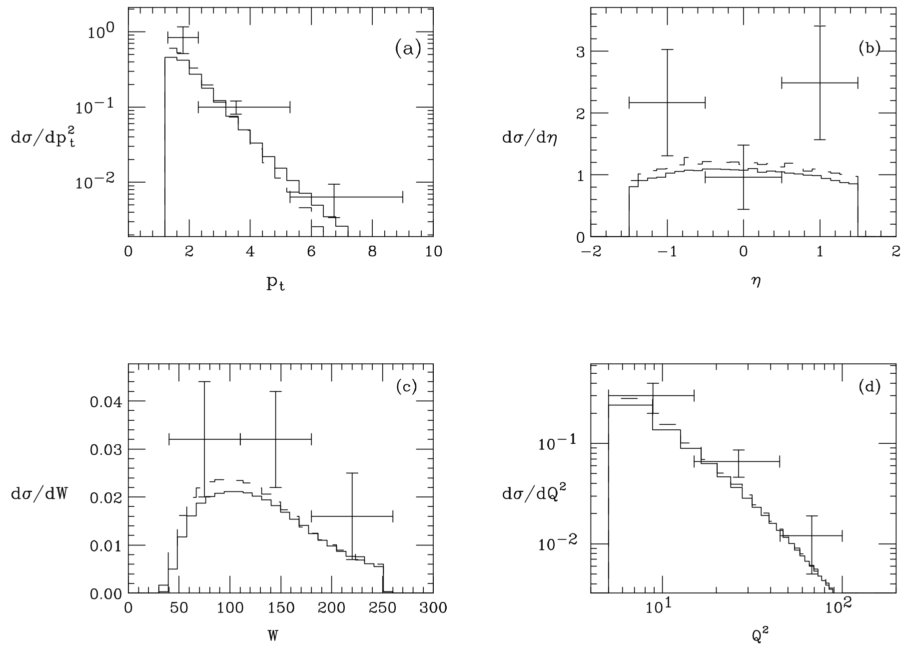

Figure 3: *Differential cross sections and ZEUS data.*

Shown in Fig. 3 are various distributions $d\sigma/dv$ for the reaction (6), where the heavy (anti)quark has fragmented into a D^* meson, with v representing (a) the D^* transverse momentum $p_T^{D^*}$ (b) its pseudorapidity η^{D^*} (c) the hadronic final state invariant mass W (d) Q^2 for the kinematic range 5 GeV^2 $< Q^2 <$ 100 GeV^2, $0 < y < 0.7$, $1.3\,\text{GeV} < p_T^{D^*} < 9\text{GeV}$ and $|\eta^{D^*}| < 1.5$. The data are from a recent ZEUS analysis [15]. The NLO theory curves have been produced by using the GRV [11] parton density set, with Peterson fragmentation [16]. The dashed line is for $\mu = 2m$, $m = 1.35$ GeV and $\epsilon = 0.035$, whereas the solid line is for $\mu = 2\sqrt{Q^2 + 4m^2}$, $m = 1.65$ GeV and $\epsilon = 0.06$. From Fig. 3 and studies in Ref. [14] it is clear that a wide range of studies can be and are being performed already at the single particle inclusive level. Preliminary conclusions [14, 15] are that the data follow the shape of the NLO predictions quite well, but lie above the theory curves. The H1 collaboration [14] has recently shown clearly from the $d\ln\sigma/dx_D$ distribution that the charm production mechanism is indeed boson-gluon fusion, (after earlier indications from the EMC collaboration [17]) as opposed to one where the charm quark is taken from the sea. Here $x_D = 2|\vec{p}_{D^*}|/W$ in the $\gamma^* P$ c.m. frame

Next we examine a few charm-anticharm correlations. At the experimental level such cor-

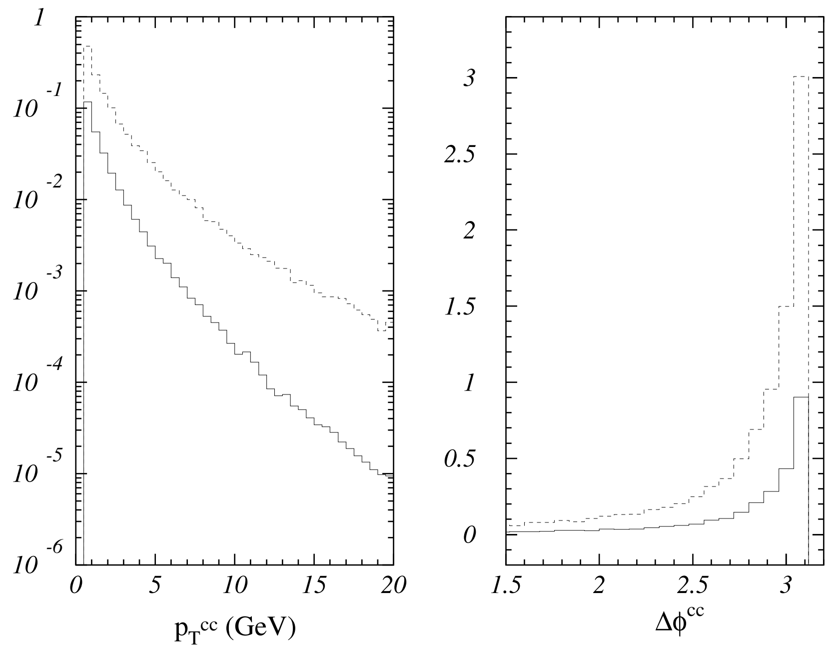

Figure 4: *Differential distributions* $dF_2(x, Q^2, m^2, p_{cc})/dp_T^{cc}$ *and* $dF_2(x, Q^2, m^2, p_{cc})/d\Delta\phi^{cc}$ *at* $x = 0.001$ *and* $Q^2 = 10$ *GeV*^{2} *(solid) and 100 GeV*^{2} *(dashed).*

relations are more difficult to measure since it requires the identification of both heavy quarks in the final state. However, with the expected large luminosity that both ZEUS and H1 will collect, such studies are likely to be done. As an example we show in Fig. 4 the p_T distribution of the pair, p_T^{cc}, and the distribution in their azimuthal angle difference, $\Delta\phi^{cc}$ in the $\gamma^* P$ c.m. frame for a particular choice of x and Q^2. For these figures we used the MRSA$'$ densities [18]. Both distributions are a measure of the recoiling gluon jet.

In summary, differential distributions of deep-inelastic heavy quark production offer a rich variety of studies of the QCD production mechanism. Fruitful experimental studies, even with low statistics, have been done [14, 15], and with a large integrated luminosity we therefore fully expect many more. We finally point out that besides a LO shower Monte Carlo program [19], now also a NLO program is available for producing differential distributions.

4 When is Charm a Parton?

We return to the inclusive case to ask the fundamental question in the title. The question can be more accurately phrased as follows: intuitively one expects that at truly large Q^2 the charm quark should be described as a light quark, i.e. as a constituent parton of the proton, whereas at small Q^2 (of order m^2) the boson-gluon fusion mechanism, in which the charm quark can only be excited by a hard scattering, is the correct description. This has been demonstrated recently by H1 [14] and ZEUS in [15]. In this subsection we examine where the transition between the two pictures occurs.

At LO this issue was investigated in [20]. A picture that consistently combines both descriptions, the so-called variable flavor number scheme, is presented and worked out to LO in [21]. Here we exhibit where the transition occurs at NLO [22]. In other words we will locate the onset of the large Q^2 asymptotic region, where the exact partonic coefficient functions of [2] are dominated by large logarithms $\ln(Q^2/m^2)$. These logarithms are controlled by the renormalization group, and, when resummed, effectively constitute the charm parton density. Here we however restrict ourselves to the onset of the asymptotics. Let us be somewhat more precise. In (4) we can rewrite e.g. all terms proportional to e_H^2 as

$$x\int_x^{zmax}\frac{dz}{z}\Big\{\Sigma(\frac{x}{z},\mu^2)H_{i,q}(z,\frac{Q^2}{m^2},\frac{m^2}{\mu^2})+G(\frac{x}{z},\mu^2)H_{i,g}(z,\frac{Q^2}{m^2},\frac{m^2}{\mu^2})\Big\} \tag{7}$$

where $G(x,\mu^2)$ is the gluon density and $\Sigma(x,\mu^2)=\sum_{i=q,\bar{q}}f_i(x,\mu^2)$ is the singlet combination of quark densities. In the asymptotic regime one may write

$$H_{i,j}^{(k)}(z,\frac{Q^2}{m^2},\frac{m^2}{\mu^2})=\sum_{l=0}^{k}a_{i,j}^{(k)}(z,\frac{m^2}{\mu^2})\ln^l\frac{Q^2}{m^2}\,. \tag{8}$$

The effort lies in determining the coefficients $a_{i,j}^{(k)}$. Similar expressions hold for the other coefficients in (4). Taking the limit of the coefficients in [2] is extremely complicated. Rather, a trick [22] was used, exploiting the close relationship of the $\ln(Q^2/m^2)$ logarithms with collinear (mass) singularities. The ingredients are the massless two-loop coefficient functions of [23] and certain two-loop operator matrix elements. The trick, dubbed "inverse mass factorization", essentially amounts to reinserting into the IR safe massless coefficient functions the collinear singularities represented by the logarithms $\ln(Q^2/m^2)$. See [22] for details.

There is another advantage to obtaining the asymptotic expresssions. The terms in eq. (4) proportional to e_L^2 have been integrated and full analytical expressions for them exist [22], but in the other terms in eq. (4) two integrals still need to be done numerically. Therefore in the large Q^2 region the asymptotic formula is able to give the same results much faster, as the latter formula needs no numerical integrations.

In Fig. 5 we show the ratio of the asymptotic to exact expressions for $F_2(x,Q^2,m^2)$ for the case of charm as a function of Q^2 for four different x values. Here the GRV [11] parton density

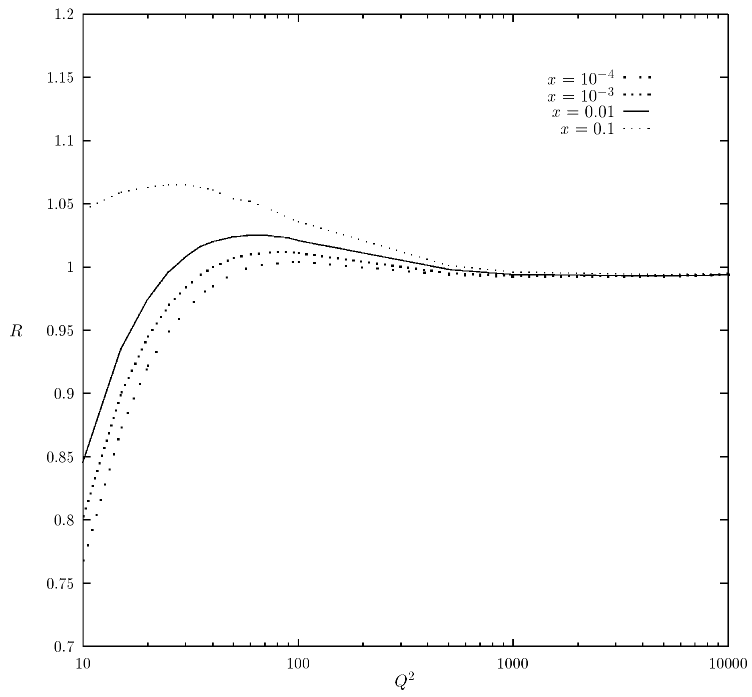

Figure 5: *Ratio of the asymptotic to exact expressions for* $F_2(x, Q^2, m^2)$ *for the case of charm.*

set was used, for three light flavors. We see that, surprisingly, already at Q^2 of order 20-30 GeV^2 the asymptotic formula is practically identical to the exact result, indicating that at these not so large Q^2 values, and for the inclusive structure function, the charm quark behaves already very much like a parton. This is in apparent contradiction with the findings [14], mentioned in the previous subsection, that the production mechanism is boson-gluon fusion, and illustrates that, interestingly, the question in the title can have a different answer for inclusive quantities than for differential distributions having multiple scales.

We finally note that with the results shown in this subsection also the first important step is made for extending the variable flavour number scheme to NLO.

5 Conclusions

In the above we have reviewed the many interesting facets of deep-inelastic production of heavy quarks. The possibility of selecting the heavy quarks among the final state particles affords a window into the heart of the scattering process, and allows tests and measurements of some of the most fundamental aspects of perturbative QCD: the direct determination of the gluon density, many and varied studies of the heavy quark production dynamics, and insight into how and when a heavy quark becomes a parton.

References

[1] R.K. Ellis and P. Nason, Nucl. Phys. **B**312 (1989) 551; J. Smith and W.L. van Neerven, Nucl. Phys. **B**374 (1992) 36.

[2] E. Laenen, S. Riemersma, J. Smith and W.L. van Neerven, Nucl. Phys. **B**392 (1993) 162.

[3] E. Laenen, S. Riemersma, J. Smith and W.L. van Neerven, Phys. Lett. **B**291 (1992) 325.

[4] E. Laenen, S. Riemersma, J. Smith and W.L. van Neerven, Nucl. Phys. **B**392 (1993) 229.

[5] S. Frixione, M. Mangano, P. Nason and G. Ridolfi, Nucl. Phys. **B**412 (1994) 225.

[6] B.W. Harris and J. Smith, Nucl. Phys. **B**452 (1995) 109; Phys. Lett. **B**353 (1995) 535.

[7] B.W. Harris, talk A05057, presented at American Physical Society, Division of Particles and Fields 1996 Meeting, Minneapolis, Minnesota, 10-15 August 1996, to appear in proceedings.

[8] S. Riemersma, J. Smith and W.L. van Neerven, Phys. Lett. **B**347 (1995) 143.

[9] H.L. Lai et al.(CTEQ Collab.), preprint MSUHEP-60426, CTEQ-604, hep-ph/9606399.

[10] H.L. Lai et al.(CTEQ Collab.), Phys. Rev. **D**51 (1995) 4763.

[11] M. Glück, E. Reya and A. Vogt, Z. Phys. **C**67 (1995) 433.

[12] A. Vogt, DESY-96-012.

[13] M. Glück, E. Reya and M. Stratmann, Nucl. Phys. **B**422 (1994) 37.

[14] C. Adloff et al. (H1 Collab.), DESY 96-138, hep-ex/9607012.

[15] ZEUS Collab., XXVIII Int. Conf. on HEP, Warsaw (1996).

[16] C. Peterson, D. Schlatter, I. Schmitt and P. Zerwas, Phys. Rev. **D**27 (1983) 105.

[17] J.J. Aubert et al. (EMC Collab.), Nucl. Phys. **B**213 (1983) 31.

[18] A. Martin, R. Roberts and W.J. Stirling, Phys. Rev. **D**51 (1995) 4756.

[19] G. Ingelman, J. Rathsman and G.A. Schuler, DESY 96-058, hep-ph/9605285.

[20] S. Riemersma and F.I. Olness, Phys. Rev. **D**51 (1995) 4746.

[21] M.A.G. Aivazis, F.I. Olness, and W.-K. Tung, Phys. Rev. **D**50 (1995) 3085; M.A.G. Aivazis, J.C. Collins, F.I. Olness, and W.-K. Tung, Phys. Rev. **D**50 (1995) 3102.

[22] M. Buza, Y. Matiounine, R. Migneron, J. Smith and W.L. van Neerven, Nucl. Phys. **B**472 (1996) 611; M. Buza, Y. Matiounine, J. Smith and W.L. van Neerven, preprint in preparation.

[23] E. Zijlstra and W.L. van Neerven, Phys. Lett. **B**272 (1991) 127 ; Nucl. Phys. **B**383 (1992) 525.